A NEW APPROACH FOR SPOT DETECTION IN TOTAL INTERNAL REFLECTION FLUORESCENCE MICROSCOPY

Seyed Hamid Rezatofighi[1,2] *, Richard Hartley*[1,3]*, William E. Hughes*[4,5]

[1] College of Engineering and Computer Science Australian National University, Canberra, Australia
[2] Quantitative Imaging Group, CSIRO Mathematics, Informatics and Statistics, North Ryde, Australia
[3] National ICT (NICTA), Australia
[4] The Garvan Institute of Medical Research, Sydney, Australia
[5] Department of Medicine, St. Vincent's Hospital, Sydney, Australia

ABSTRACT

Biological images acquired from fluorescence microscopy-based imaging techniques, such as total internal reflection fluorescence microscopy, generally contain hundreds of subcellular components, appearing in the images as bright spots. Therefore, the first step of analysis of these images usually involves the detection of these bright spots. In this paper, we propose a new approach for spot detection using the h-dome transform along with an adaptive mask obtained from regional information. Moreover, local gradient information is used in order to distinguish the spots from other structures. To evaluate the performance of our algorithm, we test it on synthetic images and also real TIRFM images and compare our results with those of two recent methods.

Index Terms— Spot detection, gray-scale morphology, *h*-dome transform, TIRFM

1. INTRODUCTION

Total internal reflection fluorescence microscopy (TIRFM) is an imaging technique that enables the selective excitation of fluorophores in a thin layer very close to a glass/water interface. This selective excitation characteristic of TIRFM has made it a powerful tool in cell biology applications where cells (aqueous) can be grown on glass. One of the most useful applications of TIRFM in cell biology is to visualize secretory granules and characterize their properties close to the basal plasma membrane at this interface. Exocytosis is a cellular process that functions to deliver cargo on secretory vesicles into or through the plasma membrane. This process involves a number of tightly regulated steps including transport, attachment, and fusion. In each step, vesicles exhibit a different dynamic behavior, which can be identified using TIRFM sequences [1].

Since vesicles are labeled with fluorescent fusion protein constructs, i.e. green fluorescent protein (GFP) [1], they are seen in the images as hundreds of small bright spots, which may appear or disappear and be static or dynamic over the frames. Moreover, due to limitations in the image acquisition process, the images are contaminated with a high level of noise. Therefore, manual detection and analysis of these spots for biologists are tedious and susceptible to error.

With the aim of automatic analysis of the exocytotic process using TIRFM sequences, several methods are proposed in the literature. However, to our knowledge, no existing method analyzes all steps of exocytosis and the previous research mostly focuses on identifying [2, 3, 4] or statistically evaluating fusion events [5]. The main purpose of this research is to propose an automatic method for analyzing the behavior of vesicles in all steps of exocytosis.

The very first stage of this analysis generally deals with the detection of the bright spots in each image sequence. The proposed method should be able robustly to detect the bright spots in an inhomogeneous background with very low signal-to-noise ratio(SNR). In this paper, we consider methods similar to those suggested for detecting bright spots in fluorescence microscopy images. In [6], the performance of several recent detection methods applied to fluorescence microscopy images, are compared. The methods are tested on synthetic images as well as real images. Of the unsupervised methods, the detectors called the *h*-dome based detection (HD) [7] and the multiscale variance-stabilizing transform (MSVST) [8] have the best results in both synthetic and real images.

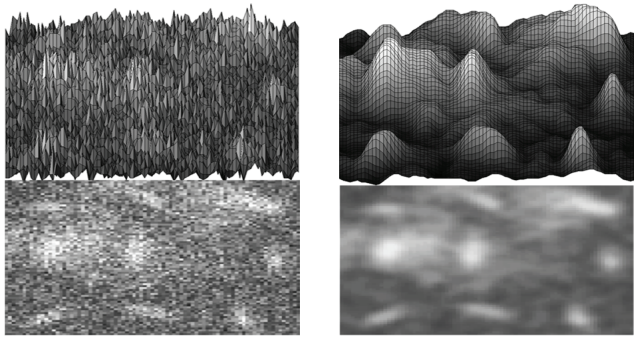
In this paper, we introduce a new approach to the *h*-dome transform based on gray-scale morphology. The proposed method designs an adaptive mask obtained from regional base information around each maximum. After applying the *h*-dome transform using the designed mask, the resulting image properly enhances the bright spots (objects) while suppressing the background noise. Finally, local gradient information is used in order to distinguish between the background structures (clutter) and the objects. To evaluate the performance of our algorithm, we test our method on the same synthetic data sets used in [6] and also real TIRFM images and compare our results with the results of the mentioned methods.

NICTA is funded by the Australian Government as represented by the Department of Broadband, Communications and the Digital Economy and the Australian Research Council through the ICT Centre of Excellence program. The authors would like to thank Dr. James G. Burchfield and Dr. Katarina Mele for usefull discussion.

2. METHOD

According to [7], the spatial intensity profile of the objects of interest can be properly modeled by a Gaussian distribution corrupted by high frequency additive noise and background structures (clutter)(Fig. 1a).

A simple approach to reducing the noise and improving the image's SNR is to smooth the image with a Gaussian kernel with variance σ^2. To avoid eliminating small objects, the scale σ must be set by the size of the smallest object. This smoothing acts as a matched filter and enhances the objects that are shaped like regional peaked domes [6].



(a) (b)

Fig. 1. Intensity profiles of (a) the original image and (b) the resulting image after applying a Gaussian kernel.

However, since the objects are located on an inhomogeneous background with various heights (intensities), it is difficult to extract them from other regional peaks, due to clutter and noise (Fig. 1b). Therefore, we use a new approach to the *h*-dome transformation based on gray-scale morphology to enhance the objects in the image.

2.1. Dome extraction using an adaptive mask

The *h*-dome transformation, first introduced by Vincent [9], is a technique that removes each object with height less than or equal to *h*, and decreases the height of the other objects by *h*. This method uses the gray-scale reconstruction algorithm defined as follows:

$$D_h(\mathcal{I}) = \mathcal{I} - \rho_{\mathcal{I}}(\mathcal{I} - h), \tag{1}$$

where the gray-scale reconstruction $\rho_{\mathcal{I}}(\mathcal{M})$ is attained by iterating gray-scale geodesic dilations of mask $\mathcal{M}$ inside $\mathcal{I}$ until stability is achieved. In the equation (1), the mask $\mathcal{M}$ is chosen as the result of subtracting a constant *h* from the image $\mathcal{I}$. Therefore, the heights of the dome structures are decreased to the amount of *h* (Fig. 2).

Unfortunately, the result of the described approach is too sensitive to the value of *h*. If a small value of *h* is chosen, all maximal structures including the objects of interest and other objects, having heights equal to or more than *h*, appear with the same height resulting in a difficulty to distinguish them (Fig. 2a). In contrast, with a large value of *h*, several peaks may be merged and therefore seen as one object, which is an undesirable result (Fig. 2b). In some cases where the objects show a significant variation in their intensities and are located in a very inhomogeneous background, no value for *h* can be found such that all objects are enhanced without merging while maintaining enough differentiation from each other.

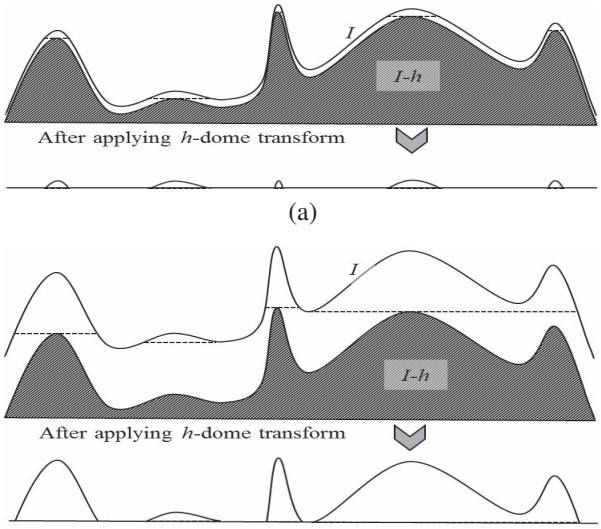


Fig. 2. A 1-D presentation of *h*-dome transform for a (a) small and (b) large value of the *h*.

In the HD method, the appropriate value for the constant *h* is determined based on the image's SNR and experimental results. However, the resulting image still includes many intersecting regions while the maximum intensity of the all objects is approximately *h* [6]. This problem becomes worse especially when the local SNR of the image noticeably changes. Therefore, in order to estimate the object positions, the method is followed by the mean-shift algorithm. Contrary to the HD method, our proposed method calculates a proper height for each object based on local information and designs an adaptive mask instead of $\mathcal{I} - h$. As a result, the method enhances all objects to their maximum possible height while avoiding intersection between objects. In order to explain the method, first, some definitions are required.

Regional Base is the nearest region around each regional maximum where the rate of decrease of intensities is noticeably low. Mathematically, the regional base $\mathcal{B}_r$ can be defined as a set of pixels (the nearest pixels) x^*_θ around a regional maximum $\mathcal{C}_p$ within a search area D_R where the gradient of the image $\mathcal{I}$ for each angle θ is minimum:

$$x^*_\theta = \underset{x \in D_R(\theta)}{\operatorname{argmin}} \|\nabla \mathcal{I}(x)\|, \tag{2}$$

where $D_R(\theta)$ is a radial line segment with the length of R starting at $\mathcal{C}_p$ and heading in the direction defined by angle θ. The radius R is set by the user to limit the search area around each regional maximum and should be bigger than the size of the biggest object of interest. Therefore, the regional base for a regional maximum is defined as:

$$\mathcal{B}_r = \{x^*_\theta | 0 \leq \theta < 2\pi\}. \quad (3)$$

Optimal Base Pixel (OBP) is the pixel $\mathcal{P}_o$ in the regional base which has maximum intensity compared to other pixels in this region.

$$\mathcal{P}_o = \underset{x \in \mathcal{B}_r}{\operatorname{argmax}}\ \mathcal{I}(x). \quad (4)$$

Maximum Possible Height (MPH) $\mathcal{H}_m$ is the difference between the intensity of the regional maximum and the intensity of its OBP.

$$\mathcal{H}_m = \mathcal{I}(\mathcal{C}_p) - \mathcal{I}(\mathcal{P}_o). \quad (5)$$

The description above calculates the maximum possible height for a single regional maximum. Therefore, the first step of our algorithm is to find the position of all candidate points (regional maxima) $\mathcal{C}_p(i), i = 1 \ldots N$ including the objects of interest and other objects in the image. To this end, equation (1) can be used with a small value of *h*. Next, the maximum possible height $\mathcal{H}_m(i)$ for each $\mathcal{C}_p(i)$ is calculated using the equations (2)-(5). Finally, the adaptive mask $\mathcal{M}_A$ is obtained by making peaks centered at the positions of regional maxima with intensity equal to $\mathcal{I}(\mathcal{C}_p(i)) - \mathcal{H}_m(i) = \mathcal{I}(\mathcal{P}_o(i))$. Applying the *h*-dome transformation (equation (1)) using this mask appropriately detects all maximal structures with their maximum possible heights.

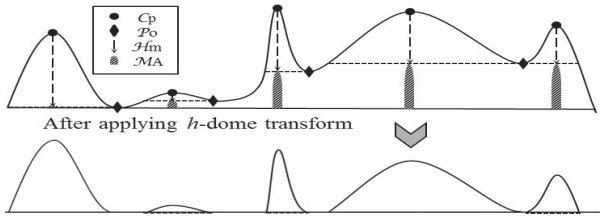


Fig. 3. A 1-D presentation of regional maxima, optimal base pixels, maximum possible heights, adaptive mask and the final enhancement result.

To decrease the processing time, here, we propose another scheme which estimates the optimal base pixel without the requirement to find the regional base. According to the above definition, the optimal base pixel can be also interpreted as follows:

1- In the radial line segment $D_R(\theta)$ starting at $\mathcal{C}_p$, the optimal base pixel is the nearest local minimum in the direction θ. Thus, a set of candidate pixels is obtained for all directions.

2- Compared to all pixels which fulfill the first condition, the optimal base pixel has the maximum intensity.

Therefore, in order to find this pixel, a growing boundary within the search area D_R, for example a circular boundary with increasing radius r ($r \leq R$), centered at $\mathcal{C}_p$ can be used. Among all pixels located on the boundary with radius r, the pixel with the maximum intensity is chosen. The OBP is the pixel where this value of the maximum intensity is minimized with respect to the index r. Since the smoothed image $\mathcal{I}$ does not include sharp changes, using this method, we can properly estimate the OBP position. This approach can be also extended for 3D images using a spherical boundary. This scheme noticeably decreases the processing time compared to the first proposed method.

2.2. Detection

The enhanced image resulting from the explained method, includes all maximal structures such as the objects of interest, noise and background structures. Since the spots (the objects of interest) in our application are domes having intensities higher than their regional backgrounds, they appear as high peaked structures in the enhanced image. Therefore, it is easy to distinguish them from noise structures, which are small peaks, using thresholding on intensity. However, background structures can possibly have intensity values as high as that of the objects of interest. But, their intensities decrease gradually at a lower rate than those of the spots [7]. Therefore, the average gradient of each structure can be a suitable discriminator for distinguishing between the objects and clutter. Finally, the spots can be detected by setting a threshold on this value.

3. EXPERIMENTAL RESULTS

The performance of the proposed detection method, the so called "maximum possible height-dome" (MPHD), was first evaluated using the same synthetic data (with ground truth) used in [6]. In this data, two types of object (round or elongated) are modeled. Each type of object is placed randomly in the images with different types of background including uniform background (type A), gradient background (type B), and non-uniform background (type C) (Fig. 4). In every experiment, 16 synthetic images (each containing 256 objects) with a very high level of poisson noise (SNR= 2) were used to compare the result of the proposed method with those of two described methods (HD and MSVST detectors).

In order to quantitatively assess the performance of the algorithms, the same performance measures reported in [6] are used in this paper. To this end, the distance between the center of each detected object and its corresponding position in ground truth was calculated. If this distance is less than 4 pixels, it is counted as a true positive (TP), otherwise the detected object is a false positive (FP). The true positive rate (TPR), the number of true positive divided by the number of objects in ground truth, and the modified false positive rate (FPR*), the number of false positive divided by the number of objects in ground truth, are the performance measures used in this paper. Furthermore, to study the sensitivity of the method to changes in threshold value, free-response receiver operating characteristic (FROC) curve is shown in Fig. 5.

In Table 1, the values of TPR at the "optimal" threshold ℓ^*_d (denoted by TPR*) are compared. The optimal threshold corresponds to the value of TPR for which the FPR*$= 0.01$. Moreover, the performance measures $S_T = -(\partial \text{TPR}/\partial \ell_d)$ and $S_F = -(\partial \text{FPR*}/\partial \ell_d)$ at $\ell_d = \ell^*_d$ [6] are also reported.

By referring to Table 1 and Fig. 5, it can be inferred that the performance of detection for the proposed method in all types of synthetic images is comparable to two other methods.

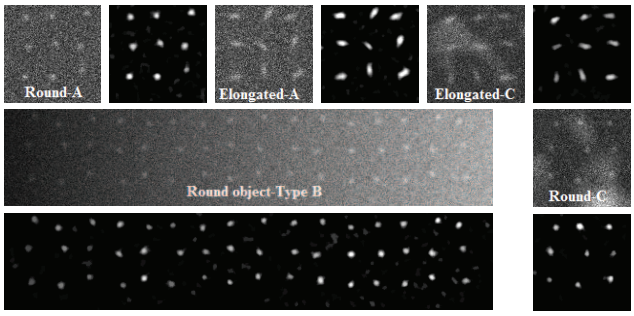


Fig. 4. Examples of different types of synthetic images at SNR= 2 and their enhancement results after applying the MPHD method.

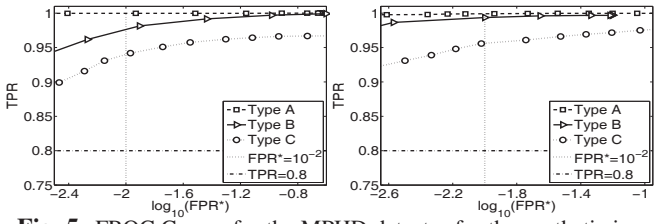


Fig. 5. FROC Curves for the MPHD detector for the synthetic images at SNR= 2 in the case of round (left) and elongated (right) objects for varying threshold.

Moreover, one of main advantages of this method is to have significantly low sensitivity to changes in threshold value as the performance measures S_T and S_F are noticeably low.

The described detection methods were also tested on two different time-lapse TIRFM sequences (Fig. 6). Since the ground truth was not available for these real data, the results of the detection were only visually evaluated by expert biologist for several sequential frames. As expected, the detection results were almost same for all the methods.

4. DISCUSSION AND CONCLUSION

In contrast with the HD method, the MSVST and MPHD methods enhance the images before the detection step, which can be helpful in the next steps of TIRF analysis, for example vesicle tracking. On the other hand, in order to use the MSVST method, several noise parameters need to be estimated from the image and if the noise parameters change, these parameters must be re-estimated [8]. In our application, the characteristics of images, such as background intensity and noise level, changes over the sequences. Further analysis on the sensitivity (not shown in this paper) shows

Image Type	Methods	Round Objects			Elongated Objects		
		TPR*	S_T	S_F	TPR*	S_T	S_F
A	MSVST	.99	.00	.01	.99	**.00**	.03
	HD	.99	.11	.05	.99	.01	.09
	MPHD	.99	**.00**	**.007**	.99	.0002	**.003**
B	MSVST	**.99**	**.00**	.02	.99	**.00**	.02
	HD	.97	.22	.05	.99	.01	.09
	MPHD	.97	.01	**.007**	.99	.007	**.007**
C	MSVST	.93	.03	.01	.96	.02	.01
	HD	.90	.21	.05	**.97**	.16	.05
	MPHD	**.94**	**.01**	**.003**	.95	**.005**	**.008**

Table 1. Optimal performance measures of the MSVST, HD, and MPHD detectors for synthetic images at SNR= 2.

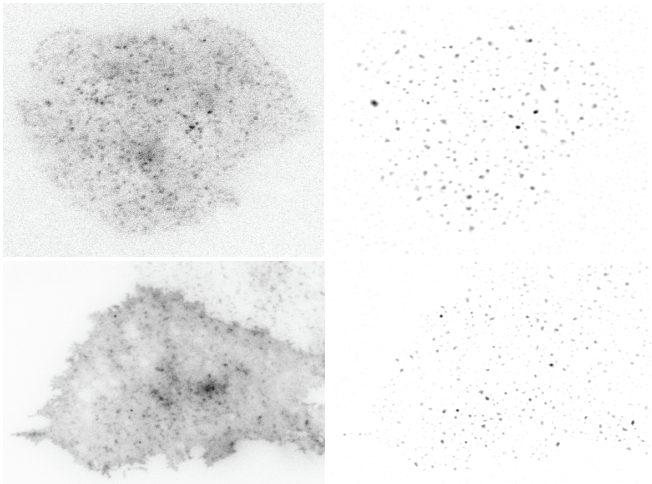


Fig. 6. Examples of two inverted real TIRFM images (left column) with their inverted enhancement results (right column) after applying the MPHD method.

that the result of MPHD method is largely insensitive to the slight changes in the parameters, including R and h. Thus, this method having the lowest sensitivity to changes in values of the parameters, is preferred for our future analysis.

5. REFERENCES

[1] J.G. Burchfield, J.A. Lopez, K. Mele, P. Vallotton, and W.E. Hughes, "Exocytotic vesicle behaviour assessed by total internal reflection fluorescence microscopy," *Traffic*, vol. 11, pp. 429–439, April 2010.

[2] K. Mele, P. Vallotton, J.G. Burchfield, D.E. James, and W.E. Hughes, "Towards fully automated identification of vesicle-membrane fusion events in TIRF microscopy," *Int. J. Computer Aided Eng. Technol.*, vol. 1, no. 4, pp. 502–515, September 2009.

[3] K. Mele, A. Coster, J.G. Burchfield, J. Lopez, D.E. James, W.E. Hughes, and P. Vallotton, "Automatic identification of fusion events in TIRF microscopy image sequences," in *Proc. IEEE Int. Conf. Computer Vision Workshops*, 2009, pp. 578–584.

[4] A. Chessel, B. Cinquin, S. Bardin, J. Boulanger, J. Salamero, and C. Kervrann, "A detection-based framework for the analysis of recycling in TIRF microscopy," in *Proc. IEEE Int. Symp. Biomed. Imag.*, 2010, pp. 1281–1284.

[5] R. Sebastian, M. E. Diaz, G. Ayala, K. Letinic, J. Moncho-Bogani, and D. Toomre, "Spatio-temporal analysis of constitutive exocytosis in epithelial cells," *IEEE/ACM Trans. Comput. Biol. Bioinf.*, vol. 3, no. 1, pp. 17–32, March 2006.

[6] I. Smal, M. Loog, W. Niessen, and E. Meijering, "Quantitative comparison of spot detection methods in fluorescence microscopy," *IEEE Trans. Med. Imaging*, vol. 29, no. 2, pp. 282–301, February 2010.

[7] I. Smal, W. Niessen, and E. Meijering, "A new detection scheme for multiple object tracking in fluorescence microscopy by joint probabilistic data association filtering," in *Proc. IEEE Int. Symp. Biomed. Imag.*, 2008, pp. 264–267.

[8] B. Zhang, J. Fadili, J.-L. Starck, and J.-C. Olivo-Marin, "Multiscale variance-stabilizing transform for mixed-poisson-gaussian processes and its applications in bioimaging," in *Proc. IEEE Int. Conf. Image Process.*, 2007, pp. VI–233–VI–236.

[9] Luc Vincent, "Morphological gray scale reconstruction in image analysis: Applications and efficient algorithms," *IEEE Trans. Image Process.*, vol. 2, no. 2, pp. 176–201, April 1993.